Leakage of holes induced by Si doping in the AlGaN first barrier layer in GaN/AlGaN multiple-quantum-well ultraviolet light-emitting diodes

Wei Liu, Shiwei Yuan, Xiaoya Fan

PII: S0022-2313(20)31773-7

DOI: https://doi.org/10.1016/j.jlumin.2020.117806

Reference: LUMIN 117806

To appear in: *Journal of Luminescence*

Received Date: 24 August 2020

Revised Date: 5 November 2020

Accepted Date: 24 November 2020

Please cite this article as: W. Liu, S. Yuan, X. Fan, Leakage of holes induced by Si doping in the AlGaN first barrier layer in GaN/AlGaN multiple-quantum-well ultraviolet light-emitting diodes, *Journal of Luminescence*, https://doi.org/10.1016/j.jlumin.2020.117806.

Leakage of holes induced by Si doping in the AlGaN first barrier layer in GaN/AlGaN multiple-quantum-well ultraviolet light-emitting diodes

Wei Liu[a,*], Shiwei Yuan[b] and Xiaoya Fan[b]

[a]*School of Microelectronics, Northwestern Polytechnical University, Xi'an, 710072, China*

[b]*School of Software, Northwestern Polytechnical University, Xi'an, 710072, China*

Abstract

The electroluminescence characteristics of GaN/AlGaN multiple-quantum-well ultraviolet light-emitting diodes (LEDs) with different concentrations of silicon impurities in the first AlGaN barrier layer near the N-type GaN region is investigated numerically. It is found that the LED's electroluminescence spectrum blueshifts and its peak intensity increases first and then decreases, as the Si-doping concentration increases. This is because that the effective potential height and width of the first barrier layer is reduced due to the screening effect by the ionization of silicon impurities. As a result, more electrons can be injected into the active region, enhancing the luminescence efficiency. However, when the impurity concentration is too high, the leakage of holes may become severe, leading to a reduction of the luminescence intensity for the most heavily doped sample at the injection current of 20 mA.

Keywords: ultraviolet LED, GaN/AlGaN multiple quantum wells, first barrier, doping concentration, screening effect.

1. Introduction

During the past decades, the GaN-based visible light-emitting diodes (LEDs), which employ the InGaN/GaN multiple-quantum-well (MQW) structure as the active region, have been successfully used in the fields of white-light illumination and color display [1-6]. Recently, the ultraviolet LED based on AlGaN material has attracted lots of attention due to its potential applications in environmental purification, disinfection, and short-distance security communication [7-10]. Nevertheless, the luminescence efficiency of AlGaN-based ultraviolet LED is still quite low at present, which is suffered from the difficult growth of high-quality AlGaN alloy [11,12], low injection rate of holes [13], leakage of electrons [14], strong quantum-confined Stark effect (QCSE) caused by polarization field [15], difficult P-type doping for AlGaN material, and the crystal defects induced by lattice mismatch in GaN/AlGaN heterostructure [16,17]. Thus, it is important to carefully study and optimize the epitaxial structures of ultraviolet LEDs as well as the crystal quality of AlGaN materials in order to enhance the device performance of ultraviolet LEDs [18-26]. Particularly, for the GaN/AlGaN MQW ultraviolet LEDs studied in this work, it is found that the AlGaN first barrier layer (FBL), which is the first layer of MQW layers and is next to the N-type GaN layer, may affect the luminescence characteristics of the ultraviolet LEDs significantly. Therefore, the influence of Si-doping concentration in FBL on the luminescence characteristics of GaN/AlGaN MQW ultraviolet LED is investigated numerically. It is found that an appropriate concentration of silicon impurities in the AlGaN FBL can improve the overall luminescence efficiency of ultraviolet LEDs. However, the excessive Si-doping concentration may lead to a degradation of the device performance by decreasing the light-emission efficiency of the first GaN quantum well next to the N-type GaN region, which is discussed in detail in this paper.

* Corresponding author: liuwei127@nwpu.edu.cn

2. Device Structure and Parameters

Fig. 1 shows the epitaxial structure of the studied GaN/AlGaN MQW ultraviolet LEDs. The LED structure is composed of a 3-μm-thick n-GaN layer with Si-doping concentration of 2×10^{18} cm^{-3} growing on the sapphire substrate, a 30-nm-thick AlGaN FBL with varied concentration of silicon impurities, an unintentionally doped MQW active region, a 100-nm-thick p-AlGaN electron blocking layer with 30% Al content, a 200-nm-thick p-$Al_{0.2}Ga_{0.8}N$ layer, and 100-nm-thick p-GaN cap layer with Mg-doping concentration of 1×10^{20} cm^{-3}. The MQW region consists of 4 pairs of 3-nm-thick GaN quantum well layers and 10-nm-thick AlGaN barrier layers with 20% Al content. To distinguish each individual GaN quantum wells conveniently, along the growth direction, the first GaN QW, which is closely next to the N-type GaN layer, is named as QW1, the second and third ones are QW2 and QW3, respectively, and the last QW near the P-type GaN layer is called as QW4. The Si-doping concentrations in the AlGaN FBL are 0, 1×10^{17}, 5×10^{17}, 1×10^{18}, 2×10^{18} and 5×10^{18} cm^{-3} for samples L0, L1, L2, L3, L4 and L5, respectively.

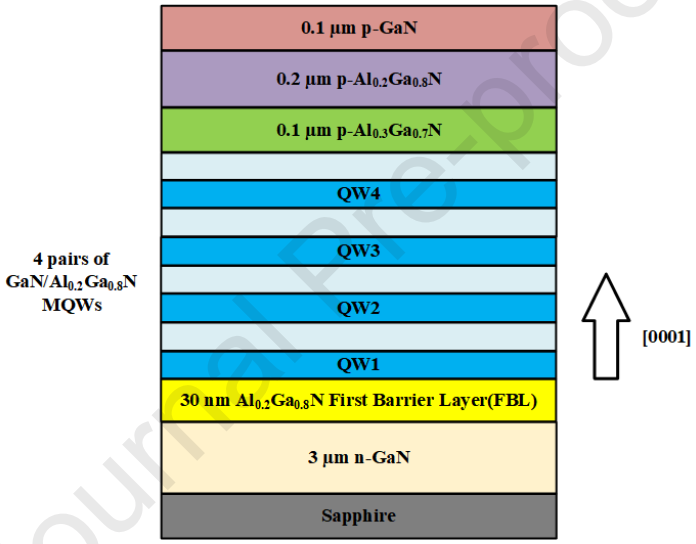

Fig. 1 Schematic structure of GaN/AlGaN MQW ultraviolet LEDs.

In this work, the device characteristics of GaN/AlGaN MQW ultraviolet LEDs are studied numerically. The energy bands of MQW active region, the radiative and nonradiative recombination processes, and the drift and diffusion formulas of carriers are solved self-consistently. There are 3 types of recombination currents in the active region, i.e., the Schockley-Read-Hall (SRH) nonradiative, the radiative, and the Auger recombination currents, where the SRH recombination lifetime is assumed to be 1 ns, the radiative recombination rate is calculated by integrating the spontaneous emission spectrum with a Lorentzian function, and the Auger recombination coefficient is set to be 1×10^{-34} $cm^{-6}\cdot s^{-1}$. The electron and hole mobilities of AlGaN are 250 and 5 $cm^2\cdot V^{-1}\cdot s^{-1}$, while those of GaN are 300 and 10 $cm^2\cdot V^{-1}\cdot s^{-1}$, respectively. The default band ratio ΔEc/ΔEv is 0.7/0.3. The interfacial charge density induced by spontaneous and piezoelectric polarization is calculated using the method proposed by Fiorentini et al [27]. Considering the possible defect factors, the interfacial charge density is assumed to be 50% of the theoretical value [28]. The studied LED device is cylindrical with a diameter of 120 μm, which is operated at room temperature. The electroluminescence (EL) properties of LED samples are mainly studied at the injection current of 20 mA, which is chosen as a typical working condition for EL measurement.

3. Results and discussions

All the LED devices show the normal forward characteristics of PN junction in the simulation. The numerical forward voltages of samples L0 to L5 are 3.464, 3.463, 3.457, 3.453, 3.449 and 3.446 V, respectively, which are basically consistent with the experimental results of LEDs with similar structures in literatures [29,30]. The slightly reduced forward voltages from samples L0 to L5 may be ascribed to the reduced effective height of FBL potential barrier for both electrons and holes due to the increased Si-doping concentration in the AlGaN FBL, which will be discussed carefully later. The EL spectra of all LED samples at 20-mA injection current are depicted in Fig. 2. It can be seen that the peak wavelengths of EL spectra decrease with increasing the concentration of silicon impurities in FBL, e.g. the EL peak wavelengths of L0, L1, L2, L3, L4 and L5 are 359.7, 359.6, 359.5, 359.2, 359.0 and 358.7 nm, respectively. Meanwhile, it is also noted that from samples L0 to L3 the peak intensity increases remarkably, but it decreases slightly from L4 to L5, as plotted in the inset in Fig. 2. In short, the EL spectra blueshift and the its peak intensity increases first and then decreases when the silicon impurities in FBL increase. In fact, it is found that the luminescence intensity of LED sample changes hardly with continuously increasing the Si-doping concentration above 5×10^{18} cm^{-3}. Thus, in order to simplify the analysis, only the samples with doping concentration less than 5×10^{18} cm^{-3} are studied in this work.

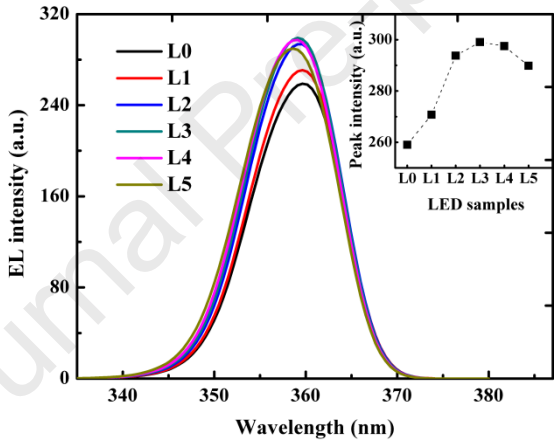

Fig. 2 EL spectra of all LED samples at the injection current of 20 mA. The inset shows the variation of EL peak intensity from samples L0 to L5.

It is known that the overall luminescence property of the MQW-based LEDs depends on the EL spectrum of each individual GaN quantum wells in the active region, and the effects of Si-doping concentration in the AlGaN FBL on the EL property may be different for different individual QWs. Therefore, the EL peak intensities and peak wavelengths of QW1, QW2, QW3 and QW4 in all LED samples are extracted and exhibited in Fig. 3.

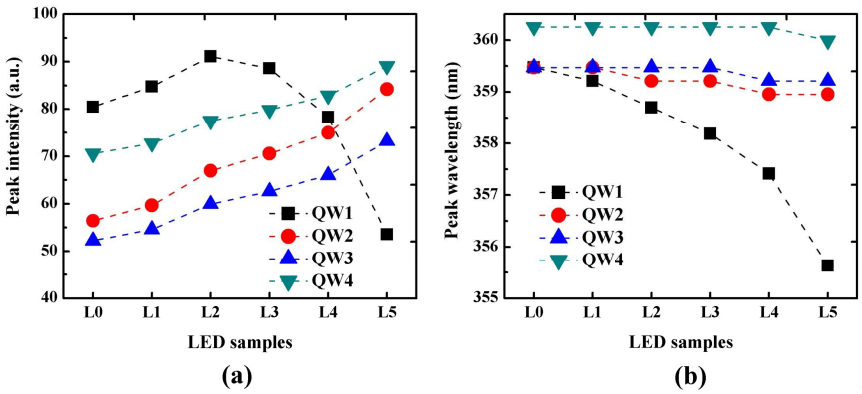

Fig. 3 Variations of peak intensities (a) and peak wavelengths (b) of each individual GaN QWs at the injection current of 20 mA.

From Fig. 3(a) it is seen that the EL peak intensities of QW2, QW3 and QW4 are enhanced monotonically with increasing Si-doping concentration. However, the peak intensity of QW1 increases first and then decreases obviously. Compared with Fig. 2, it is found that for the whole LED devices the spectral intensity of sample L4 is the maximum, while the intensity of QW1 reaches the maximum for sample L2. The reason is that although the peak intensity of QW1 reduces from samples L2 to L5, those of other QWs increase monotonically as shown in Fig. 3(a). As a result, the overall EL intensity of LED samples doesn't decrease until the Si-doping concentration exceeds 2×10^{18} cm^{-3}, since the peak intensity of QW1 reduces significantly for the highly doped sample L5 with the impurity concentration of 5×10^{18} cm^{-3} in FBL.

On the other hand, the EL spectral peak wavelengths of all QWs blueshift as the concentration of silicon impurities increases in AlGaN FBL, as shown in Fig. 3(b). It is noticed that from samples L0 to L5 the reduction of peak wavelength is 3.5 nm for QW1, while it is less than 1 nm for other QWs, i.e. the spectral blueshift of QW1 is more significant. The spectral blueshift of LED devices is 1.1 nm in Fig. 2 from samples L0 to L5. The extent of spectral blueshift of LED samples is between those of QW1 and other QWs, since the overall spectral properties of MQW LED devices are determined by the superposition of the luminescence spectra of each individual GaN QWs.

To gain a deeper understanding on the variations of EL spectra of each individual QWs, the distributions of electrons and holes in MQW active region at the injection current of 20 mA are plotted in Fig. 4 for all samples. It can be seen from Fig. 4(a) that the increase of electron concentration in QW1 is remarkable, while it is slight in the other 3 QWs. However, in Fig. 4(b) it is surprising to find that the hole concentration in QW1 is reduced significantly, while those in other QWs are almost unchanged, as the concentration of silicon impurities in AlGaN FBL increases. Therefore, from samples L0 to L5, the EL peak intensities of QW2, QW3 and QW4 increase monotonically as shown in Fig. 3(a), since the concentrations of electron increases slightly and those of holes keep almost constant in the three QWs. For the case of QW1, the EL intensity increases from samples L0 to L2 with doping concentration of 5×10^{17} cm^{-3}, since the reduction of hole concentration is less significant than the increase of electron concentration. However, from samples L3 to L5, i.e. the Si-doping concentration exceeds 5×10^{17} cm^{-3}, although the electron concentration still increases in QW1, the hole concentration decreases remarkably, which causes an obvious reduction of the luminescence intensity of QW1. As a result, the EL peak intensity of QW1 increases from samples L0 to L2 and then decreases from L3 to L5, as depicted in Fig. 3(a).

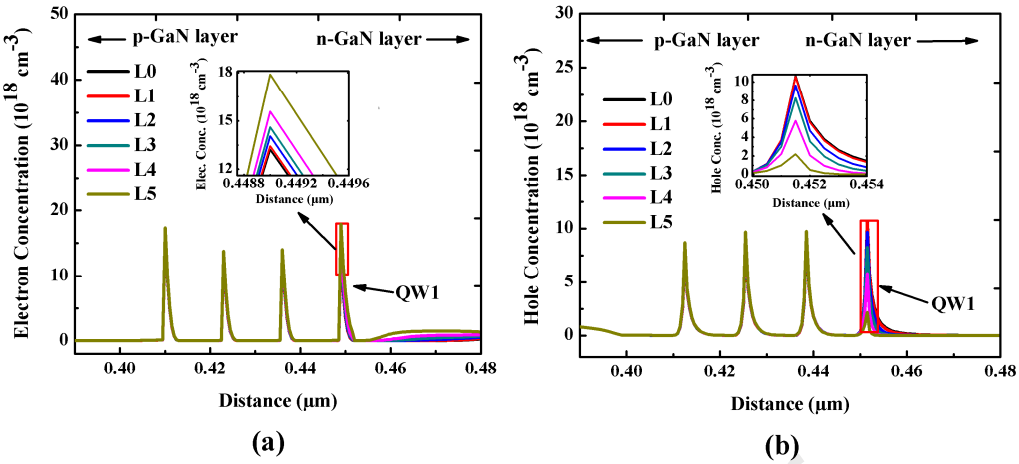

Fig. 4 Distributions of electrons (a) and holes (b) in each individual GaN QWs for all samples at the injection current of 20 mA.

According to the carrier distributions, it is considered that the polarization field in GaN QWs can be partially screened by the increased electrons injected in the GaN QWs, which may be the main reason responsible for the EL spectral blueshift for QW2, QW3 and QW4 in Fig. 3(b). In addition, it should be pointed out that the polarization charges caused by the lattice mismatch at the interface of GaN/AlGaN heterostructure can be partially screened by the free electrons ionized by the silicon impurities in AlGaN barrier layers [31,32]. Therefore, for the case of QW1, when the concentration of silicon impurities in the AlGaN FBL increases, the ionized free electrons can effectively screen the polarization charges at the interface between GaN QW1 and AlGaN FBL. As a consequence, combined with the increased concentration of injected electrons in QW1 and the ionization of silicon impurities in FBL, the polarization-induced electric field in QW1 is weakened significantly, leading to a remarkable blueshift of the EL spectrum for QW1 as shown in Fig. 3(b).

Fig. 5 shows the energy band diagrams of the MQW layers without bias current to further discuss the distributions of carriers in different QWs. For the ideal undoped FBL, e.g. sample L0, both the conduction and valance bands of FBL are tilted, forming triangular potential barriers hindering the diffusions of electrons and holes, respectively. In other words, the electrons and holes need to overcome the triangular FBL barriers to enter into QW1 and N-type GaN layers, respectively. When the Si-doping concentration increases, the electric field in FBL decreases due to the screening effect of free electrons generated by the ionization of silicon impurities. As a result, the tilt of FBL energy bands becomes less significant. For the heavily doped LEDs, such as sample L5, the most parts of the energy bands in the FBL area are almost flat, as seen in Fig. 5.

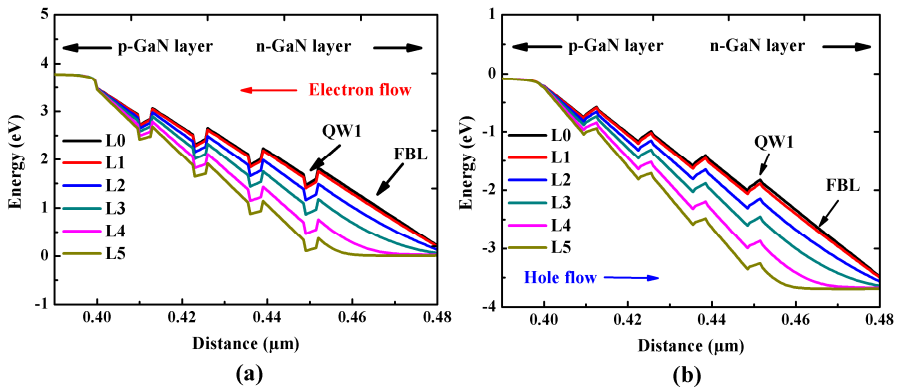

Fig. 5 Conduction (a) and valence bands (b) of MQW active region for all samples at zero bias.

For the electrons, when the concentration of silicon impurities increases, the conduction band of FBL becomes less tilted in Fig. 5(a). The effective height of the triangular potential barrier of AlGaN FBL, which is defined as the distance between the highest and the lowest points of the conduction band in the AlGaN FBL area, is reduced. For instance, the electronic effective barrier heights of AlGaN FBL are 1910, 1853, 1624, 1341, 936 and 554 meV for samples L0, L1, L2, L3, L4 and L5, respectively. Furthermore, accompanied with the reduction of the effective barrier height, the triangular barrier of AlGaN FBL becomes narrowed due to the screening effect, as seen in Fig. 5(a). The width of FBL triangular barrier for the heavily doped sample L5, for example, is less than 5 nm. According to the basic theory of quantum mechanics, the thinner barrier can facilitate the quantum tunneling effect, which makes more electrons injected into QW1 from the N-type GaN region [33]. Therefore, the reductions of both effective height and width of triangular potential barrier in the conduction band of AlGaN FBL may jointly cause more electrons injected from the N-type GaN layer into QW1 as well as the whole MQW layers.

Similar to the electrons in conduction band, the effective height of FBL potential barrier for holes can be defined as the difference between the highest and lowest points of the valence band in the AlGaN FBL area. Due to the screening effect induced by the ionized silicon impurities, the effective barrier height for holes monotonically decreases from 1687 to 367 meV with increasing the Si-doping concentration in FBL. Since the holes are injected from the MQW active region into the N-type GaN region, the FBL is used to prevent holes entering the N-type region. Therefore, the reduction of effective height barrier of AlGaN FBL in valance band actually weakens the blocking effect of FBL on holes, which may cause a large number of holes leak from the QW1 into the N-type GaN layer.

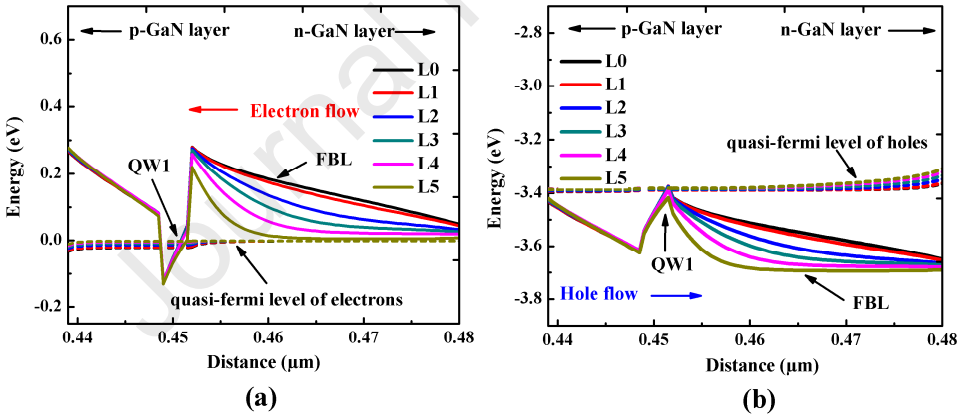

Fig. 6 Conduction (a) and valence bands (b) of QW1 and FBL for all samples at the injection current of 20 mA.

To further discuss the transport of electrons and holes under forward bias condition, the energy band diagrams of the area near QW1 and FBL at the injection current of 20 mA are plotted in Fig. 6. Similar to the analysis of energy bands at zero bias, for the electrons in the conduction band in Fig. 6(a), it is obvious that both the effective height and width of the triangular potential barriers of AlGaN FBL decrease with increasing doping concentration, which can facilitate the injection of more electrons from N-type layers into QW1 as well as the whole MQW region. For the holes in the valance band in Fig. 6(b), the effective barrier height of AlGaN FBL, which is 290 meV for sample L0, is reduced to 278 meV for sample L5. Meanwhile, as the Si-doping concentration increases in FBL, the effective distance between QW1 and N-type region becomes short, i.e. the FBL barrier for holes is narrowed. Therefore, the leakage of holes may become significant for the heavily doped sample L5.

Combined with Figs. 5 and 6, it is reasonable that in Fig. 4 the electron concentration in the MQW layers increases monotonously with increasing the silicon impurities in FBL, and especially the

increase in QW1 is the most significant, while there is a sharp reduction of hole concentration in QW1 for the highly doped sample at the injection current of 20 mA.

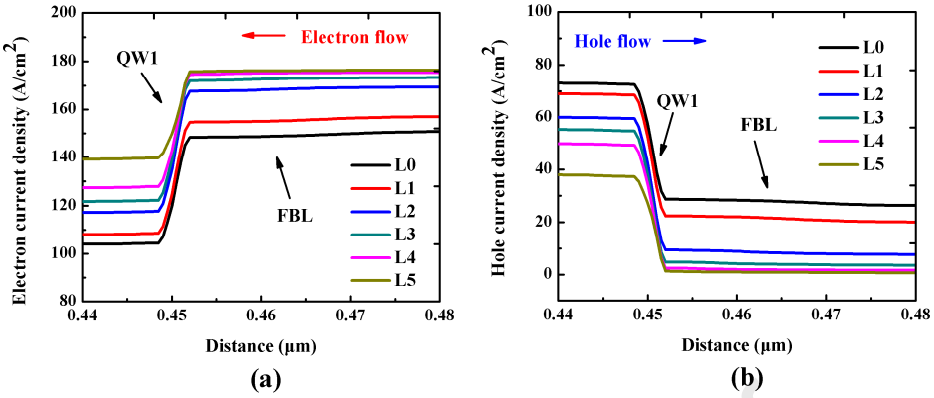

Fig. 7 Current densities of electrons (a) and holes (b) in the n-side of all LED samples at the injection current of 20 mA.

Fig. 7 demonstrates the numerical distribution of electron and hole currents in the regions of QW1 and FBL for all samples at 20-mA injection current. It is commonly known that more charge carriers can contribute to a larger current density. Thus, in Fig. 7(a) it is obvious that the electron current density in QW1 increases with increasing the silicon impurities in FBL, which is consistent with the increased electron concentration in QW1 in Fig. 4(a). On the contrary, in Fig. 7(b) the hole current density in QW1 decreases from samples L0 to L5 remarkably, which accords with the reduction of hole concentration in QW1 in Fig. 4(b). These results indicate that as the Si-doping concentration increases, more electrons can be injected from N-type region into QW1, while more holes may leak outside from QW1 into N-type region, due to the weakened blocking effect of FBL on both electrons and holes.

According to the aforementioned discussions, the doping of silicon impurities in AlGaN FBL can screen the electric field and weaken the blocking effect of FBL on both electrons and holes, which cause the increase of electrons and the reduction of holes in QW1, respectively. For the lightly doped samples, the increase of electrons is more significant, facilitating to improve the EL intensity of the whole LED. However, when the doping concentration of silicon impurities in FBL is too high, the hole concentration in QW1 may decrease significantly, since the remarkably increased electrons ionized by the heavily doped silicon impurities may weaken the blocking effect of FBL on holes intensely. As a result, the luminescence efficiency of QW1 is deteriorated severely, which may reduce the EL intensity of the whole MQW ultraviolet LEDs, such as sample L5.

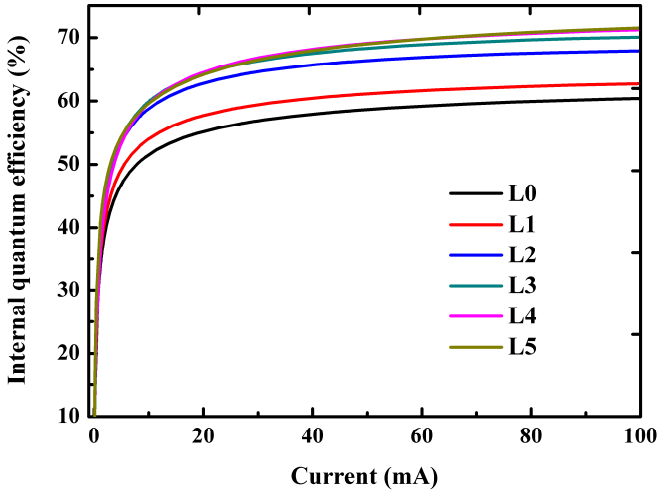

Fig. 8 Internal quantum efficiency versus injection currents for all samples in the range from 0 to 100 mA.

At last, the effects of Si-doping concentration in FBL on the droop behaviors of LED samples are studied in Fig. 8 which shows the dependence of internal quantum efficiency (IQE) on the injection currents. It can be seen that the IQE values of all samples reduce hardly as the current increases even to 100 mA. It implies that the droop behaviors of our LED devices can be ignored in the current range studied. On the other hand, in general the values of IQE are improved from samples L0 to L3, while those of samples L3, L4 and L5 are almost equal to each other. Especially, at the injection current of 20 mA, the IQE value of samples L4 is slightly larger than that of L5, which is consistent with the comparison of peak intensities of EL spectra in Fig. 2. However, when the injection current increases to 100 mA, the IQE value becomes a little larger for sample L5 than L4. This is because that the transport capability of holes is worse than that of electrons due to the much larger effective mass for holes. Therefore, compared with the rapid increase of electrons in QW1 with increasing current, the increase of hole leakage is slow relatively. In other words, for the highly doped sample, at very high currents the hole leakage may be less effective, while the increase of electrons in QW1 is more significant. As a consequence, the IQE of sample L5 becomes slightly larger than that of L4 at the high injection current of 100 mA.

4. Conclusion

In summary, the effects of Si-doping concentration in the AlGaN FBL on the luminescence characteristics of GaN/AlGaN MQW ultraviolet LEDs are studied numerically. It is found that when the concentration of silicon impurities increases, the EL peak wavelengths of LED samples reduce monotonously, while peak intensities increase first and then decrease. It is considered that the increased silicon impurities in FBL can weaken the FBL blocking effect on both electrons and holes, which may make the electron concentration in the MQW layers increased and correspondingly improve the LED's luminescence intensity. However, for the heavily doped sample, the blocking effect of FBL on holes is significantly weakened, leading to a serious hole leakage outside from QW1. As a result, the luminescence efficiency of QW1 decreases significantly due to the severe reduction of hole concentration in QW1, which may deteriorate the overall EL intensity of the LED sample. Therefore, it is suggested that the proper silicon doping in the AlGaN FBL is beneficial to improve the performance of GaN/AlGaN MQW ultraviolet LEDs. However, the excessive doping may lead to the severe leakage of holes, and eventually cause the degradation of the device performance.

Acknowledgments

The authors acknowledge the support from National Natural Science Foundation of China (Grant No. 62074129), Natural Science Foundation of Shaanxi Province (Grant No. 2019JM-452), and Fundamental Research Funds for the Central Universities.

References

[1] Z. Wang, X.Y. Shan, X.G. Cui, P.F. Tian, Characteristics and techniques of GaN-based micro-LEDs for application in next-generation display, J. Semicond. 41 (2020) 041606.

[2] M.H. Chang, D. Das, P.V. Varde, M. Pecht, Light emitting diodes reliability review, Microelectron. Reliab. 52 (2012) 762-782.

[3] M. Manikandan, D. Nirmal, J. Ajayan, P. Mohankumar, P. Prajoon, L. Arivazhagan, A review of blue light emitting diodes for future solid-state lighting and visible light communication applications, Superlattices Microstruct. 136 (2019) 106294.

[4] C. Xu, C.D. Zheng, X.M. Wu, S. Pan, X.G. Jiang, J.L. Liu, F.Y. Jiang, Effects of V-pits covering layer position on the optoelectronic performance of InGaN green LEDs, J. Semicond. 40 (2019) 052801.

[5] F. Liang, J. Yang, D.G. Zhao, Z.S. Liu, J.J. Zhu, P. Chen, D.S. Jiang, Y.S. Shi, H. Wang, L.H. Duan, L.Q. Zhang, H. Yang, Room-temperature continuous-wave operation of GaN-based blue-violet laser diodes with a lifetime longer than 1000 h, J. Semicond. 40 (2019) 022801.

[6] Q.L. Liu, Y.J. Feng, H.J. Tian, X.Y. He, A.Q. Hu, X. Guo, Fabrication of flexible AlGaInP LED, J. Semicond. 41 (2020) 032302.

[7] M. Kneissl, TY. Seong, J. Han, H. Amano, The emergence and prospects of deep-ultraviolet light-emitting diode technologies, Nat. Photonics. 13 (2019) 233-244.

[8] B. Asma, H. Abdelkader, Numerical simulation of UV LEDs with GaN and BGaN single quantum well, J. Semicond. 40 (2019) 032802.

[9] H. Hirayama, N. Maeda, S. Fujikawa, S. Toyoda, N. Kamata, Recent progress and future prospects of AlGaN-based high-efficiency deep-ultraviolet light-emitting diodes, Jpn. J. Appl. Phys. 53 (2014) 100209.

[10] M. Kneissl, T. Kolbe, C. Chua, V. Kueller, N. Lobo, J. Stellmach, A. Knauer, H. Rodriguez, S. Einfeldt, Z. Yang, NM. Johnson, M. Weyers, Advances in group III-nitride-based deep UV light-emitting diode technology. Semicond. Sci. Technol. 26 (2011) 014036.

[11] J.S. Park, J.K. Kim, J. Cho, T.Y. Seong, Review group III-nitride-based ultraviolet light-emitting diodes: ways of increasing external quantum efficiency, ECS J. Solid State Sci. Technol. 6 (2017) Q42-Q52.

[12] M.A. Khan, E. Matsuura, Y. Kashima, H. Hirayama, Influence of undoped-AlGaN final barrier of MQWs on the performance of lateral-type UVB LEDs, Phys. Status Solidi A-Appl. Mat. 216 (2019) 1900185.

[13] W.Y. Lin, T.Y. Wang, S.L. Ou, J.H. Liang, D.S. Wu, Improved performance of 365-nm LEDs by inserting an un-doped electron-blocking layer, IEEE Electron Device Lett. 35 (2014) 467-469.

[14] F. Mehnke, C. Kuhn, M. Guttmann, C. Reich, T. Kolbe, V. Kueller, A. Knauer, M. Lapeyrade, S. Einfeldt, J. Rass, T. Wernicke, M. Weyers, M. Kneissl, Efficient charge carrier injection into sub-250nm AlGaN multiple quantum well light emitting diodes, Appl. Phys. Lett. 105 (2014) 051113.

[15] J. Brault, D. Rosales, B. Damilano, M. Leroux, A. Courvill, M. Korytov, S. Chenot, P. Vennegues, B. Vinter, P. De Mierry, A. Kahouli, J. Massies, T. Bretagnon, B. Gil, Polar and semipolar GaN/Al0.5Ga0.5N nanostructures for UV light emitters, Semicond. Sci. Technol. 29 (2014) 084001.

[16] D.B. Li, K. Jiang, X.J. Sun, C.L. Guo, AlGaN photonics: recent advances in materials and ultraviolet devices, Adv. Opt. Photonics, 10 (2018) 43-110.

[17] M. Ali, O. Svensk, L. Riuttanen, M. Kruse, S. Suihkonen, A.E. Romanov, P.T. Torma, M. Sopanen, H. Lipsanen, M.A. Odnoblyudov, V.E. Bougrov, Enhancement of near-UV GaN LED light extraction efficiency by GaN/sapphire template patterning, Semicond. Sci. Technol. 27 (2012) 082002.

[18] M.R. Kwon, T.H. Park, T.H. Lee, B.R. Lee, T.G. Kim, Improving the performance of AlGaN-based deep-ultraviolet light-emitting diodes using electron blocking layer with a heart-shaped graded Al composition, Superlattices Microstruct. 116 (2018) 215-220.

[19] X.M. Chen, Y.A. Yin, D.N. Wang, G.H. Fan, Investigation of AlGaN-based deep-ultraviolet light-emitting diodes with AlInGaN/AlInGaN superlattice electron blocking layer, J. Electron. Mater. 48 (2019) 2572-2576.

[20] R.K. Mondal, V. Chatterjee, S. Pal, Efficient carrier transport for AlGaN-based deep-UV LEDs

wth graded superlattice p-AlGaN, IEEE Trans Electron Devices. 67 (2020) 1674-1679.

[21] H.B. Yu, D. Chen, Z.J. Ren, M. Tian, S.B. Long, J.N. Dai, C.Q. Chen, H.D. Sun, Enhanced performance of an AlGaN-based deep-ultraviolet LED having graded quantum well structure, IEEE Photon. J. 11 (2019) 8201006.

[22] H. Li, C.J. Chang, S.Y. Kuo, H.C. Wu, H.M. Huang, T.C. Lu, Improved performance of near UV GaN-based light emitting diodes with asymmetric triangular multiple quantum wells, IEEE J. Quantum Electron. 55 (2019) 3200104.

[23] Y. Li, Z.H. Xing, Y.L. Zheng, X. Tang, W.T. Xie, X.F. Chen, W.L. Wang, G.Q. Li, High-efficiency near-UV light-emitting diodes on Si substrates with InGaN/GaN/AlGaN/GaN multiple quantum wells, J. Mater. Chem. C. 8 (2020) 883-888.

[24] H.P. Hu, S.J. Zhou, X.T. Liu, Y.L. Gao, C.Q. Gui, S. Liu, Effects of GaN/AlGaN/Sputtered AlN nucleation layers on performance of GaN-based ultraviolet light-emitting diodes, Sci. Rep. 7 (2017) 44627.

[25] R.X. Ni, C.C. Chuo, K. Yang, Y.J. Ai, L. Zhang, Z. Cheng, Z. Liu, L.F. Jia, Y. Zhang, AlGaN-based ultraviolet light-emitting diode on high-temperature annealed sputtered AlN template, J. Alloys Compd. 794 (2019) 8-12.

[26] N. Susilo, E. Ziffer, S. Hagedorn, L. Cancellara, C. Netzel, NL. Ploch, S.J. Wu, J. Rass, S. Walde, L. Sulmoni, M. Guttmann, T. Wernicke, M. Albrecht, M. Weyers, M. Kneissl, Improved performance of UVC-LEDs by combination of high-temperature annealing and epitaxially laterally overgrown AlN/sapphire, Photonics Res. 8 (2020) 589-594.

[27] V. Fiorentini, F. Bernardini, O. Ambacher, Evidence for nonlinear macroscopic polarization in III-V nitride alloy heterostructures, Appl. Phys. Lett. 80 (2002) 1204-1206.

[28] F.Z. Li, L.S. Wang, G.J. Zhao, Y.L. Meng, H.J. Li, S.Y. Yang, Z.G. Wang, Performance enhancement of AlGaN-based ultraviolet light-emitting diodes by inserting the last quantum well into electron blocking layer, Superlattices Microstruct. 110 (2017) 324-329.

[29] J. Han, M.H. Crawford, R.J. Shul, J.J. Figiel, A.V. Nurmikko, AlGaN/GaN quantum well ultraviolet light emitting diodes, Appl. Phys. Lett. 73 (1998) 1688-1690.

[30] C.Q. Chen, V. Adivarahan, J.W. Yang, M. Shatalov, E. Kuokstis, M.A. Khan, Ultraviolet light emitting diodes using non-polar a-plane GaN-AlGaN multiple quantum wells, Jpn. J. Appl. Phys. Part II 42 (2003) L1039-L1040.

[31] V. Fiorentini, F. Bernardini, F. Della Sala, A. Di Carlo, P. Lugli, Effects of macroscopic polarization in III-V nitride multiple quantum wells, Phys. Rev. B. 60 (1999) 8849-8858.

[32] K.K. Tian, Q. Chen, C.S. Chu, M.Q. Fang, L.P. Li, Y.H. Zhang, W.G. Bi, C.Q. Chen, Z.H. Zhang, J.N. Dai, Investigations on AlGaN-based deep-ultraviolet light-emitting diodes with Si-doped quantum barriers of different doping concentrations, Phys Status Solidi-R. 12 (2018) 1700346.

[33] Ajit Kumar, *Fundamentals of Quantum Mechanics*, Cambridge University Press (Cambridge, UK) p. 88.

Highlights

1. Effects of Si-doping concentration in the first barrier layer (FBL) are studied.
2. LED’s luminescence intensity increases first and then decreases with increasing Si.
3. The injection of electrons is enhanced with increasing Si-doping concentration.
4. The leakage of holes is significant for the highly doped sample.
5. Blocking effects on electrons and holes are weakened with increasing Si impurities.

Author Statement

The authors state that the idea and results discussed in this paper is original, and there is no plagiarism, no repeated publication in our manuscript.

Prof. Wei Liu proposed the idea and performed the sample modeling and data analysis. Dr. Shiwei Yuan performed the simulations, Prof. Xiaoya Fan participated the discussions. The whole work is supervised by Prof. Wei Liu.

All authors contribute to the manuscript and agree with this article.

Prof. Wei Liu, Dr. Shiwei Yuan, and Prof. Xiaoya Fan

Northwestern Polytechnical University

127 West Youyi Road, Beilin District, Xi'an Shaanxi

710072, People's Republic of China

Conflict of Interest

The authors confirm that there is no any conflict of interest in this manuscript.

Wei Liu